The influence of DOC and UVR on the genomic integrity of *Daphnia magna*

Raoul Wolf*, Tom Andersen, Dag O. Hessen, and Ketil Hylland

Department of Biosciences, University of Oslo, Oslo, 0316 Norway

*Correspondence author. E-mail: raoul.wolf@ibv.uio.no

Summary

1. Many northern freshwaters are currently experiencing a pronounced "browning", i.e., an increase of terrestrially derived dissolved organic carbon (DOC). Chromophoric DOC offers protection against photodamage by absorbing harmful ultraviolet radiation (UVR), but may also produce free radicals and reactive oxygen species (ROS) following photoactivation. The aim of this study was to explore the combined effects of DOC and UVR on DNA integrity of limnetic zooplankton. Specifically, DNA strand breaks in the cladoceran *Daphnia magna* were investigated.

2. DNA strand breaks were assessed using comet assays with treatment of individual daphnids. A four-by-four design was used for exposure to DOC (2.03, 5, 10, and 20 mg L^{-1}), UVA (0, 10.8, 21.7, and 43.4 μmol m^{-2} s^{-1} at 390 nm), and their combinations. ROS production from photoactivated DOC was quantified using a modified DCFH-DA *in vitro* ROS detection assay.

3. While UVA had no effects on DNA damage above background levels (4.5 to 2.8%), we observed increased DNA damage in DOC treatments (4.1 to 9.1%). The highest increase was observed in combined DOC and UVA treatments (up to 20.2%). ROS production showed similar patterns, as simultaneous exposure to both DOC and UVA resulted in higher formation rates than exposure to DOC and UVA alone (up to 684.5 μmol L^{-1} versus 5.9 to 13.1 and 27.5 to 83.9 μmol L^{-1}, respectively). This indicates that the observed increase in DNA damage was due to ROS production of photoactivated DOC.

4. This study showed that strong interactive effects of short-wave radiation and DOC could have major genomic impacts on pelagic biota. With future scenarios of increased DOC, our study points towards increasing oxidative stress for ecosystems.

These findings highlight an important aspect of climate change at the intersection between ecology, limnology and toxicology.

Key-words: Browning, climate change, dissolved organic carbon, DNA damage, photoactivation, ROS formation, ultraviolet radiation, zooplankton

Introduction

Water browning, i.e., an increase of dissolved organic carbon (DOC) in freshwater systems is a known phenomenon throughout the northern hemisphere (Solomon et al. 2015). Potential drivers of this browning include changes in agriculture (Evans et al. 2012), altered vegetation (Larsen, Andersen & Hessen 2011), climate change (Erlandsson et al. 2008), and decreased sulphuric deposition (Monteith et al. 2007). This poses a multitude of impacts on physical, chemical, and biological properties in lakes (Williamson et al. 2015). DOC attenuates shortwave light, which has both negative (light attenuation, various photoproducts) and positive effects (nutrient release, photoprotection) for primary producers (Palen et al. 2002; Kelly et al. 2014; Thrane, Hessen & Andersen 2014; Karlsson et al. 2015; Seekell, Lapierre & Karlsson 2015). Photoactivated DOC is known to release free radicals and reactive oxygen species (ROS; Cooper & Zika 1983; Scully, McQueen & Lean 1996; Richard et al. 2007), which may induce membrane and DNA damages in plankton (Cooke et al. 2003; Vehmaa et al. 2013).

While stratospheric ozone depletion is a major factor for increasing ultraviolet radiation (UVR) on earth (Dugo, Han & Tchounwou 2012; IPCC 2014; Robinson & Erickson III 2015), the impact of UVR on lake biota is first and foremost regulated by the concentration of chromophoric DOC. While current browning will increase attenuation and narrow down the zone of active photochemistry, drought may work in the opposite direction and increase water clarity and UVR penetration due to extended renewal rates and reduced terrestrial inputs of DOC (Yan et al. 1996; Schindler et al. 1997). Zooplankton may be affected by UVR by increased mortality (Zagarese, Tartarotti & Añón Suárez 2003), reduced fecundity and growth (Williamson et al. 1994; de Lange et al. 1999), or synergistic effects in combination with chemical

stressors (Hessen & Alstad Rukke 2000; Ma, Brennan & Diamond 2012). Underlying these phenotypic fitness costs are, however, cellular damages. The UVR-mediated damage is generally caused by direct photon damage (MacFayden et al. 2004), but also by photoactivation of DOC, producing free radicals and harmful ROS like peroxides, superoxides, singlet oxygen, and hydroxide radicals (Cooper et al. 1988; Fede & Grannas 2015). While UVB photons are more efficient in producing these ROS (Cullen & Neale 1994; IPCC 2014), UVA is the main contributor to their formation in natural systems, as most UVB is absorbed in the stratosphere (Cooper et al. 1994; Abele-Oeschger, Tüg & Röttgers 1997).

In a scenario of moderate browning, the net impact of DOC on zooplankton could be considered positive, if photoprotection outweighs decreased primary production (Hessen et al. 2004). However, indirect effects of DOC, like ROS formation under UVR-exposure, could have a negative impact on zooplankton in the upper layers. UVR affects zooplankton species *via* a range of direct and indirect mechanisms (Williamson et al. 2001; Hessen, Borgeraas & Ørbæk 2002; MacFayden et al. 2004; Scoville & Pfrender 2010). E.g., UVR is a main cue for vertical migration of zooplankton species during daytime (Leech & Williamson 2001; Rhode, Pawlowski & Tollrian 2001), a driving force in phenotypic divergence (Miner & Kerr 2011; Miner et al. 2015), and a potent DNA disruptor (Malloy et al. 1997). DNA damaging effects of UVR and other mutagenic drivers to zooplankton species like *Daphnia* are well established (Pellegri, Gorbi & Buschini 2014; Tartarotti et al. 2014), but the indirect effects of UVR *via* formation of free radicals and ROS under gradients of DOC is less explored.

This study seeks to investigate the interaction of DOC and UVR exposure on DNA damage in *Daphnia magna* STRAUS, 1820. Using orthogonal study designs with

environmentally relevant levels of DOC and UVR, both ROS production and resulting DNA damage were determined. As proxy for DNA damage, strand breaks were chosen. Although UVR and ROS result in different initial DNA modifications (e.g., pyrimidine dimers and oxidised nucleotides, respectively), they subsequently induce enzyme-mediated DNA strand breaks, allowing for a comparative analysis of DNA damage (Collins et al. 1997; Collins 2009).

Materials and methods

DAPHNIA MAGNA CULTURING

The *D. magna* culture was kept in multiple aerated 15–20 L full silicate glass aquaria at a temperature of 20±1 °C. Filtered tap water (0.22 µm polyethersulfone sterilising filter; Corning, Corning, NY, USA) was used as medium, enriched to 4 mmol $CaCl_2$ L^{-1}, 4 mmol $NaHCO_3$ L^{-1}, and 12 nmol H_2SeO_3 L^{-1}, with additional vitamins (4 nmol B_{12} L^{-1}, 2 nmol D-biotin L^{-1}, and 300 nmol thiamine HCl L^{-1}) and pH = 7.5. The light:dark cycle was set to 16:8 h (L 18 W/950 fluorescent lamps; OSRAM, Munich, Germany) and *Daphnia* were fed *ad libitum* with the chlorophyte *Chlamydomonas reinhardtii* P.A. DANGEARD, 1888. The *D. magna* culture (DHI strain) was obtained from Norwegian Institute for Water Research (NIVA; Oslo, Norway) in early 2014. It has since been kept at our facilities without observable signs of stress (e.g., decreased reproduction or ephippia).

GRADIENTS IN DISSOLVED ORGANIC CARBON (DOC) AND ULTRAVIOLET RADIATION (UVR)

DOC gradients were produced with lyophilized natural organic matter (NOM) from Lake Skjervatjern in Western Norway, which was isolated by reverse osmosis and subsequently freeze-dried (details in Hessen & Færøvig 2001). Concentrations of 2.03, 5, 10, and 20 mg DOC L^{-1} were prepared in *D. magna* culture medium and verified on a TOC-V_{CPH} Total Organic Carbon Analyzer (Shimadzu, Kyoto, Japan). 2.03 mg DOC L^{-1} was the background concentration of DOC in *D. magna* culture medium. UVR exposure was conducted using a fully programmable 96-LED board (Microwell 96 LED Controller, Version 3.2, 13.06.2014;

https://www.tindie.com/stores/Dead_Bug_Prototypes/; Dead_Bug_Prototypes, Sandnes, Norway) at 390 nm (UVA_{390}) and photon fluxes of 0, 10.8, 21.7, and 43.4 μmol m^{-2} s^{-1}. Photon flux gradients were scripted in Arduino (version 1.6.6; https://www.arduino.cc/en/Main/Software/) and calibrated using a SpectraPen LM 500-UVIS spectroradiometer (Photon Systems Instruments, Drásov, Czech Republic). Unless noted otherwise, all chemicals were purchased from Sigma-Aldrich (St. Louis, MO, USA).

IN-VIVO D. MAGNA EXPOSURE

A four-by-four bifactorial geometric design was chosen, using DOC concentrations and UVA_{390} intensities mentioned above. This reflected typical ranges of DOC concentrations in boreal lakes and surface water intensities of UVR (Larsen et al. 2011). Exposures were performed in black deep 96-well plates (Advantage 2mL, Square Top/V Bottom, Black 96-Well Collection Plate; Analytical Sales and Services, Pompton Plains, New Jersey, USA) to avoid scattering of UVA_{390} between wells. For each DOC×UVA_{390} combination, three five-day old daphnids were exposed individually for six hours. The experiment was repeated three times, yielding nine analyses per treatment in total.

COMET ASSAY PROCEDURE

The comet assay is a single cell gel electrophoresis, allowing detection of DNA strand breaks of single nuclei (Singh et al. 1988). Here, a modified high-throughput protocol for multiple agarose gels on a hydrophilic polyester film was used (Gutzkow et al. 2013). After exposure, individual daphnids were rapidly transferred into 1.5 mL Eppendorf tubes filled with 50 μL ice-cold buffer P (8.5 mmol NaH_2PO_4 L^{-1}, 91.5

mmol Na_2HPO_4 L^{-1}, 100 mmol NaCl L^{-1}, 1 mmol EDTA L^{-1}, 2 wt% citric acid, and pH = 7.8; Pellacani et al. 2006) and homogenized. The homogenate was diluted 1:10 in 0.75 wt% ultra-low gelling temperature agarose (Type IX-A) in PBS (137 mmol NaCl L^{-1}, 2.7 mmol KCl L^{-1}, 10 mmol Na_2HPO_4 L^{-1}, 2 mmol KH_2PO_4 L^{-1}, and 10 mmol EDTA L^{-1}) at 20 °C and 20 µL of the mixture were transferred onto the hydrophilic side of a GelBond film (Lonza, Basel, Switzerland). Films were placed in ice-cold lysis buffer (2.5 mol NaCl L^{-1}, 100 mmol EDTA L^{-1}, 10 mmol Tris L^{-1}, 10 vol% DMSO, 1 vol% Triton X-100, and pH = 10) and kept therein overnight. Films were rinsed in electrophoresis buffer (300 mmol NaOH L^{-1}, 1 mmol EDTA L^{-1}, and 6 vol% concentrated HCl) for 20 min before electrophoresis was run at 15 V for 25 min. Afterwards, films were transferred to neutralising buffer (400 mmol Tris L^{-1} and pH = 7.5) at room temperature for 15 min, before rinsing in dH_2O and dehydration in ethanol for 2 h. Films were air-dried overnight in darkness. Staining was done with 1×SYBR Gold (Life Technologies, Carlsbad, California, USA) in TE buffer (10 mmol Tris L^{-1}, 1 mmol EDTA L^{-1}, and pH = 8) for 20 min, then the films were rinsed in dH_2O and mounted. Comets were scored on a Nikon Eclipse LV 100ND microscope with a Nikon Plan Fluor 20×/0.50 objective (Nikon Corporation, Tokyo, Japan) using Comet Assay IV software (version 4.3; Perceptive Instruments, Bury St Edmund, England, UK). DNA damage was defined as percentage tail DNA and 50 comets were scored for each daphnid.

QUANTIFICATION OF ROS PRODUCTION

To quantify *in vitro* ROS production, a four-by-three bifactorial design was applied, using 2.03, 5, 10, and 20 mg DOC L^{-1} and 0, 21.7, and 43.4 µmol UVA_{390} m^{-2} s^{-1}. DOC concentrations were achieved by diluting NOM powder in *D. magna* culture

medium and UVA_{390} intensities were calibrated as described above. ROS production was determined colourmetrically using 2',7'-dichlorofluorescin diacetate (DCFH-DA; CAS 4091-99-0). The principle mechanism is described in Fig. S1 (Marchesi et al. 1999; Gomes, Fernandes & Lima 2005). Experiments were carried out in black 96-well plates (Nunc 96F Nontreated MicroWell; Thermo Scientific Fisher, Roskilde, Denmark) to avoid scattering of UVA_{390} across wells. Each well contained 100 µL DOC medium with 25 µmol DCFH-DA L^{-1} and 20 U esterase (from porcine liver; CAS 9016-18-6). A hydrogen peroxide (H_2O_2) standard was used (0.03–72.1 nmol L^{-1}) and substituted the DOC medium where applicable. Five replicates were used for each DOC×UVA_{390} combination and three for each H_2O_2 concentration. Plates were incubated at 20±0.3 °C for six hours. Fluorescence was measured on a BioTek Synergy Mx plate reader with Gen5 software (version 1.10.8; BioTek Instruments, Winooski, VT, USA) and the experiment repeated three times.

ABSORBED PHOTON FLUX

The relationship between ROS formation rates and absorbed photon fluxes of UVA_{390} was investigated with absorbed photon flux C in mol m^{-3} s^{-1} calculated as

$$\frac{\mathrm{d}C}{\mathrm{d}t} = \frac{q_{\mathrm{p},\lambda}\left[1 - 10^{-abs(\lambda)}\right]}{V} \cdot A$$

where $q_{\mathrm{p},\lambda}$ is the photon flux in mol m^{-2} s^{-1}, $abs(\lambda)$ the exposure absorbance at 390 nm (non-dimensional), V the exposure volume in m^3, and A the exposure area in m^2 (IUPAC 2006). Absorbance values for the same DOC×UVA_{390} treatments used for

ROS production estimation were measured on a BioTek Synergy Mx plate reader and Gen5 software (version 1.10.8; BioTek Instruments) at 390 nm.

Absorbed photons at the end of the experiment were calculated by multiplying the absorbed photon flux with the exposure time.

STATISTICAL ANALYSES

Statistical analyses were carried out using open source statistical software R (version 3.3.1; R Core Team 2016) and recommended package nlme (version 3.1-128; Pinheiro et al. 2016).

DNA damage data was aggregated by median values of 50 scored comets for each animal (Collins et al. 2014) and analysed in LME models using individual daphnids and experimental replicates as random factors with individual daphnids nested within experimental replicates, DNA damage as response variable, and DOC, UVA_{390}, and their combination as fixed effects. This LME model was also used for three-dimensional visualisation of DNA damage in relation to DOC and UVA_{390}. As DNA damage data was skewed, it was power-transformed ($\lambda = 0.5$) to improve error distribution.

For analysis of ROS production, measured fluorescence was aggregated by mean values of five technical replicates, standardised to H_2O_2 fluorescence and analysed using an LME model with power-transformed ($\lambda = 0.5$) ROS production as response variable, DOC, UVA_{390}, and absorbed photons (substituting DOC×UVA_{390} interactions) as fixed effects, and experimental replicates as random factor.

To investigate the correlation of ambient ROS production and DNA damage in *D. magna*, a reduced major axis regression approach was applied. Two separate LME models were fitted: (1) untransformed DNA damage as response variable, mean ROS

production as fixed effect, and individual daphnids and experimental replicates as random factors with individual daphnids nested within experimental replicates, and (2) untransformed ROS production as response variable, mean DNA damage as fixed effect, and experimental replicates as random factor. The final regression was calculated as the geometric mean of both fixed-effects estimates and their confidence intervals (Sprent & Dolby 1980). The effect of ROS production on DNA damage was analysed using model (1) with power-transformed ($\lambda = 0.5$) DNA damage data.

For each LME model, *P* values of fixed-effect model parameters were calculated using Wald *F*-tests with marginal (type III) sum of squares (Pinheiro & Bates 2000; Li & Redden 2015) and a significance threshold of $P < 0.05$.

Results

THE EFFECTS OF DOC AND UVA ON DNA DAMAGE IN *D. MAGNA*

DOC had an effect on DNA strand breaks in *D. magna* (Tab. 1). While UVA_{390} did not yield a significant effect, the co-exposure surpassed DOC-induced strand break levels. The DOC effect on DNA damage was significant ($F_{1,129} = 10.45$, $P < 0.01$), while effects of UVA_{390} were not significant ($F_{1,129} = 2.20$, $P > 0.05$). The results also showed a strong interactive effect of DOC and UVA_{390} on DNA damage ($F_{1,129} = 11.86$, $P < 0.001$; Fig. 1).

ROS PRODUCTION AND CORRELATION WITH DOC, UVA AND ABSORBED PHOTONS

Absorbed photons and UVA_{390} induced *in vitro* ROS production (Tab. 2). At single exposures, ROS production was significantly affected by UVA_{390} ($F_{1,30} = 14.79$, $P < 0.001$), but not by DOC ($F_{1,30} = 3.42$, $P > 0.05$). *In-vitro* ROS production was strongly correlated with the amount of absorbed photons ($F_{1,30} = 98.13$, $P < 0.001$). Additionally, a distinct “grouping” was observed, seemingly dependent on UVA_{390} intensities (Fig. 2).

DNA DAMAGE IN *D. MAGNA* AS A RESULT OF ROS PRODUCTION

The data for ROS production allowed for a collapse of dimensions, i.e., DOC and UVA_{390} could be expressed as ROS production, which had a strong effect on DNA damage in daphnids ($F_{1,95} = 57.41$, $P < 0.001$; Fig. 3).

Discussion

THE DNA-DAMAGING POTENTIAL OF ABIOTIC ROS PRODUCTION

This present study demonstrated a strong, interactive effect of DOC and UVA_{390} on ROS formation rates and that *de novo* ROS formation is mediated by photoactivated DOC. At environmentally relevant levels of DOC and UVA_{390}, the generated ROS caused significant increases in DNA damage in *D. magna*.

ROS formation was mainly promoted by the interaction of DOC and UVA_{390}, with the amount of absorbed photons providing a mechanistic explanation for this interaction (Fig. 2). Interestingly, UVA_{390} had an effect on ROS formation by itself, while there was no significant generation by DOC. Possible explanations include autocatalytic processes, in which already existing ROS could evoke the production of additional ROS from DOC as second-order effects of UVA_{390} photons (Wilson, Hinman & Sheridan 2000), ROS release of UVA_{390}-activated container material, or other synergistic interactions (Howard & Webster 2009). Overall, the ROS formation rates reported in this study surpassed previous estimated H_2O_2 formation rates from lake systems (e.g., Scully et al. 1996), most likely because our results presented a gross ROS formation rate as opposed to a H_2O_2 formation rate alone. Apart from H_2O_2, other ROS are generally extremely short-lived and many of the produced ROS would react immediately with nearby organic matter before interacting with *Daphnia*. While ROS formation rate and DNA damage were still proportional, only a fraction of the formed ROS was thus responsible for the observed DNA damage. Although *D. magna* possess enzymatic repair abilities for DNA base dimers (photolyase; Thoma 1999) or replacement of entire nucleotides (excision repair; Sinha & Häder 2002),

these pathways do not repair DNA strand breaks, as detected in the comet assay of our study.

While comet assay data sets contained some scatter (Tab. 1), variations of this magnitude are considered part of natural variability among individuals (Martins & Costa 2015). Indeed, the resolution of individual *Daphnia* in the comet assay resulted in a more scattered, yet more holistic view of DNA damage, theoretically allowing for investigation of individual-, treatment-, and experiment-variability (Frenzilli, Nigro & Lyons 2009; David et al. 2011). Furthermore, the low background damage in controls suggests a high sensitivity of the assay in this study (Jha 2008; Pellegri, Gorbi & Buschini 2014). The DOC-induced increase in DNA damage could possibly be due to the presence of polycyclic aromatic hydrocarbons (PAHs) or similar compounds in the NOM, which are known to induce DNA strand breaks (e.g., Farmer et al. 2003; Fu et al. 2012).

ENVIRONMENTAL IMPLICATIONS OF DOC-MEDIATED ROS PRODUCTION FOR ZOOPLANKTON

The UVA_{390} intensities used in this study correspond to UV index number 1 or "low exposure" (Lucas et al. 2006). Intensities of this magnitude are frequently reached and surpassed in both the northern and southern hemisphere (Rae et al. 2001; Lucas et al. 2006; IPCC 2014). Data on spectral attenuation along a gradient of DOC in 75 Nordic lakes (Thrane et al. 2014) shows that UVA_{390} is mostly absorbed within the first meter of water, depending on DOC concentrations. This has implications for zooplankton residing in the upper layers of lakes or in shallow ponds, if sufficient DOC is present. In fact, for long-lived ROS, i.e., H_2O_2, the whole mixed layer could be affected by photoproducts formed in the surface layers.

297 UVA is known to be the major driver of peroxide formation in surface waters
298 (Cooper et al. 1994; Abele-Oeschger et al. 1997; Wilson et al. 2000). While UVB has
299 higher peroxide formation efficiencies than UVA, the amount of UVA photons
300 impacting on surface waters far surpasses that of UVB photons (Cullen & Neale
301 1994; IPCC 2014). This implies that the first meter of surface waters is most affected
302 by DOC-mediated ROS formation in general, and hence increasing browning
303 indicates additional oxidative stress. As UVA radiation at intensities similar to this
304 study would appear throughout the year (Rae et al. 2001; Hudson, Dillon & Somers
305 2003; Lucas et al. 2006), plankton residing in such an oxidative stress environment
306 would need to adapt, e.g., by increased enzymatic activity of oxidative stress enzymes
307 (Borgeraas & Hessen 2002).
308 To protect themselves from harmful effects of direct exposure to UVR,
309 zooplankton also uses enzymatic DNA repair and pigmentation such as melanin or
310 carotenoids (Hessen & Sørensen 1990). Some zooplankton species use mycosporine-
311 like amino acids (MAAs; Sommaruga & Garcia-Pichel 1999; Tartarotti et al. 2004;
312 Moeller et al. 2005) for UV-protection, but *Daphnia* species are not known to contain
313 MAAs (Miner et al. 2015). While carotenoids may serve a dual role by direct
314 protection, but also as radical scavengers (Mortensen et al. 1997; Skibsted 2012),
315 pigments would generally not protect well against ambient ROS. Pigments mainly
316 appear in daphnids' carapace, while ambient ROS would most likely be taken up
317 through filter-feeding ingestions or respiratory processes. On the other hand,
318 behavioural strategies such as vertical migration (Hansson & Hylander 2009) would
319 protect against both direct (photodamage) and indirect (ROS formation) effects of
320 UVR.

For zooplankton in clear-water lakes, UV radiation causes a conspicuous vertical migration, also in the absence of fish predators, to avoid DNA damage due to radiation (Williamson et al. 2001; Kessler et al. 2008). However, our results indicate that DNA damage as a result of oxidative stress in the environment could function as an additional cue for vertical migration. On an ecosystem level, the mutual effects of browning and UVR are not straightforward, since the photoprotective role of DOC in fact may be offset by damage caused by photoproducts. This interplay of such antagonistic and synergistic effects requires a detailed knowledge of the system itself (Urabe et al. 2002; Häder et al. 2007).

Increased oxidative stress could also pose an energetic trade-off for zooplankton, e.g., a reallocation of resources for UV-protecting pigments to an improved enzymatic oxidative stress response. This could result in either an increased sensitivity or tolerance towards chemical stressors causing oxidative stress. Interestingly, browning is linked to an increased abundance and mobility of anthropogenic contaminants (e.g., heavy metals and persistent organic pollutants; Bundschuh & McKie 2015). Furthermore, humic substances are known to affect the epigenome of *Daphnia* species (Menzel et al. 2011), suggesting additional mechanisms by which DOC can potentially influence zooplankton life history (Mirbahai & Chipman 2014).

In some regions, climate change will cause drier climate, less export of DOC, and extended renewal rates, causing increased water transparency and UV-stress (Yan et al. 1996; Schindler et al. 1997). In other regions, wetter climate and more terrestrial vegetation will play in concert with reduced sulphate deposition, all promoting browning of surface waters (Lapierre, Seekell & del Giorgio 2015). In both cases, better knowledge of DOC and UVR interplay is demanded to predict future ecosystem responses.

Acknowledgements

We are grateful to Berit Kaasa and Lilla Varga for assistance in DOC quantification.

Data accessibility

All data was used in the article. Additional information on the DCFH-DA assay, raw data files, and R scripts for data analysis are included in the Supporting information.

References

Abele-Oeschger, D., Tüg, H. & Röttgers, R. (1997) Dynamics of UV-driven hydrogen peroxide formation on an intertidal sandflat. *Limnology and Oceanography*, **42**, 1406–1415.

Borgeraas, J. & Hessen, D.O. (2002) Variations of antioxidant enzymes in *Daphnia* species and populations as related to ambient UV exposure. *Hydrobiologia*, **477**, 15–30.

Bundschuh, M. & McKie, B.G. (2015) An ecological and ecotoxicological perspective on fine particulate organic matter in streams. *Freshwater Biology*, **in press**, 12 p.

Collins, A.R., Dobson, V.L., Dušinská, M., Kennedy, G. & Štětina, R. (1997) The comet assay: what can it really tell us? *Mutation Research*, **375**, 183–193.

Collins, A.R. (2009) Investigating oxidative DNA damage and its repair using the comet assay. *Mutation Research*, **681**, 24–32.

Collins A.R., El Yamani, N., Lorenzo, Y., Shaposhnikov, S., Brunborg, G. & Azqueta, A. (2014) Controlling variation in the comet assay. *Frontiers in Genetics*, **5**, 1–6.

Cooke, M.S., Evans, M.D., Dizdaroglu, M. & Lunec, J. (2003) Oxidative DNA damage: mechanisms, mutation, and disease. *The FASEB Journal*, **17**, 1195–1214.

Cooper, W.J. & Zika, R.G. (1983) Photochemical formation of hydrogen peroxide in surface and ground waters exposed to sunlight. *Science*, **220**, 711–712.

Cooper, W.J., Zika, R.G., Petasne, R.G. & Plane, J.M.C. (1988) Photochemical formation of H_2O_2 in natural waters exposed to sunlight. *Environmental Science and Technology*, **22**, 1156–1160.

375 Cooper, W.J., Shao, C., Lean, D.R.S., Gordon, A.S. & Scully, Jr., F.E. (1994) Factors
376 affecting the distribution of H_2O_2 in surface waters. *Advances in Chemistry*, **237**,
377 391–422.
378 Cullen, J.J. & Neale, P.J. (1994) Ultraviolet radiation, ozone depletion, and marine
379 photosynthesis. *Photosynthesis Research*, **39**, 303–320.
380 David, R.M., Dakic, V., Williams, T.D., Winter, M.J. & Chipman, J.K. (2011)
381 Transcriptional responses in neonate and adult *Daphnia magna* in relation to
382 relative susceptibility to genotoxicants. *Aquatic Toxicology* **104**, 192–204.
383 de Lange, H.J., Verschoor, A.M., Gylstra, R., Cuppen, J.G.M. & van Donk, E. (1999)
384 Effects of artificial ultraviolet-B radiation on experimental aquatic microcosms.
385 *Freshwater Biology*, **42**, 545–560.
386 Dugo, M.A., Han, F. & Tchounwou, P.B. (2012) Persistent polar depletion of
387 stratospheric ozone and emergent mechanisms of ultraviolet radiation-mediated
388 health dysregulation. *Reviews on Environmental Health*, **27**, 103–116.
389 Erlandsson, M., Buffam, I., Fölster, J., Laudon, H., Temnerud, J., Weyhenmeyer,
390 G.A. & Bishop, K. (2008) Thirty-five years of synchrony in the organic matter
391 concentrations of Swedish rivers explained by variation in flow and sulphate.
392 *Global Change Biology*, **14**, 1191–1198.
393 Evans, C.D., Jones, T.G., Burden, A., Ostle, N., Zieliński, P., Cooper, M.D.A.,
394 Peacock, M., Clark, J.M., Oulehle, F., Cooper, D. & Freeman, C. (2012) Acidity
395 controls on dissolved organic carbon mobility in organic soils. *Global Change*
396 *Biology* **18**, 3317–3331.
397 Fede, A. & Grannas, A.M. (2015) Photochemical production of singlet oxygen from
398 dissolved organic matter in ice. *Environmental Science and Technology*, **49**,
399 12808–12815.

400 Frenzilli, G., Nigro, M. & Lyons, B.P. (2009) The comet assay for the evaluation of
401 genotoxic impact in aquatic environments. *Mutation Research/Reviews in Mutation*
402 *Research*, **681**, 80–92.
403 Gomes, A., Fernandes, E. & Lima, J.L.F.C. (2005) Fluorescence probes used for
404 detection of reactive oxygen species. *Journal of Biochemical and Biophysical*
405 *Methods*, **65**, 45–80.
406 Gutzkow, K.B., Langleite, T.M., Meier, S., Graupner, A., Collins, A.R. & Brunborg,
407 G. (2013) High-throughput comet assay using 96 minigels. *Mutagenesis*, **28**, 333–
408 340.
409 Hansson, L.A. & Hylander, S. (2009) Effects of ultraviolet radiation on pigmentation,
410 photoenzymatic repair, behavior, and community ecology of zooplankton.
411 *Photochemical and Photobiological Sciences*, **8**, 1266–1275.
412 Hessen, D.O. & Sørensen, K. (1990) Photoprotective pigmentation in alpine
413 zooplankton populations. *Aqua Fennica*, **20**, 165–170.
414 Hessen, D.O. & Alstad Rukke, N. (2000) UV radiation and low calcium as mutual
415 stressors for *Daphnia*. *Limnology and Oceanography*, **45**, 1834–1838.
416 Hessen, D.O. & Færøvig, P.J. (2001) The photoprotective role of humus-DOC for
417 *Selenastrum* and *Daphnia*. *Plant Ecology*, **154**, 263–273.
418 Hessen, D.O., Borgeraas, J. & Ørbæk, J.B. (2002) Responses in pigmentation and
419 anti-oxidant expression in Arctic *Daphnia* along gradients of DOC and UV
420 exposure. *Journal of Plankton Research*, **24**, 1009–1018.
421 Hessen, D.O., Blomqvist, P., Dahl-Hansen, G., Drakare, S. & Lindström, E.S. (2004)
422 Production and food web interactions of Arctic freshwater plankton and responses
423 to increased DOC. *Archiv für Hydrobiologie*, **159**, 289–307.

Howard, G.J. & Webster, T.F. (2009) Generalized concentration addition: a method for mixtures containing partial agonists. *Journal of Theoretical Biology*, **259**, 469–477.

Hudson, J.J., Dillon, P.J. & Somers, K.M. (2003) Long-term patterns in dissolved organic carbon in boreal lakes: The role of incident radiation, precipitation, air temperature, southern oscillation and acid deposition. *Hydrology and Earth System Sciences*, **7**, 390–398.

Häder, D.-P., Kumar, H.D., Smith, R.C. & Worrest, R.C. (2007) Effects of solar UV radiation on aquatic ecosystems and interactions with climate change. *Photochemical and Photobiological Sciences*, **6**, 267–285.

IPCC (2014) Climate change 2014: Synthesis report. Contribution of working groups I, II and III to the fifth assessment report of the *International Panel on Climate Change* (eds The Core Writing Team, R.K. Pachauri & L.A. Meyer), 151 p. IPCC, Geneva, Switzerland. https://ipcc.ch/report/ar5/syr/

IUPAC (2006) Absorbed (spectral) photon flux density. *Compendium of Chemical Terminology* (eds. M. Nic, J. Jirat & B. Kosata), p. 11. Blackwell Scientific Publications, Oxford.

Jha, A.N. (2008) Ecotoxicological applications and significance of the comet assay. *Mutagenesis*, **23**, 207–221.

Karlsson, J., Bergström, A.-K., Byström, P., Gudasz, C., Rodríguez, P. & Hein, C. (2015) Terrestrial organic matter input suppresses biomass production in lake ecosystems. *Ecology*, **96**, 2870–2876.

Kelly, P.T., Solomon, C.T., Weidel, B.C. & Jones, S.E. (2014) Terrestrial carbon is a resource, nut not a subsidy, for lake zooplankton. *Ecology*, **95**, 1236–1242.

448 Kessler, K., Lockwood, R.S., Williamson, C.E. & Saros, J.E. (2008) Vertical
449 distribution of zooplankton in subalpine and alpine lakes: ultraviolet radiation, fish
450 predation, and the transparency-gradient hypothesis. *Limnology and*
451 *Oceanography*, **53**, 2374–2382.
452 Lapierre, J.-F., Seekell, D.A. & del Giorgio, P.A. (2015) Climate and landscape
453 influence on indicators of lake carbon cycling through spatial patterns in dissolved
454 organic carbon. *Global Change Biology*, **21**, 4425–4435.
455 Larsen, S., Andersen, T. & Hessen, D.O. (2011) Climate change predicted to cause
456 severe increase of organic carbon in lakes. *Global Change Biology*, **17**, 1186–
457 1192.
458 Leech, D.M. & Williamson C.E. (2001) *In situ* exposure to ultraviolet radiation alters
459 the depth distribution of *Daphnia*. *Limnology and Oceanography*, **46**, 416–420.
460 Li, P. & Redden, D.T. (2015) Comparing denominator degrees of freedom
461 approximations for the generalized linear mixed model in analysing binary
462 outcome in small sample cluster-randomized trials. *BMC Medical Research*
463 *Methodology*, **15**, 1–12.
464 Lucas, R., McMichael, T., Smith, W. & Armstrong, B. (2006) Solar ultraviolet
465 radiation: Global burden of disease from solar ultraviolet. *Environmental burden of*
466 *disease series, No. 13* (eds A. Prüss-Üstün, H. Zeeb, C. Mathers, & M. Repacholi),
467 258 p. World Health Organisation, Geneva, Switzerland.
468 https://www.who.int/uv/health/solaruvradfull_180706.pdf
469 Ma, H., Brennan, A. & Diamond, S.A. (2012) Photocatalytic reactive oxygen species
470 production and phototoxicity of titanium dioxide nanoparticles are dependent on
471 the solar ultraviolet radiation spectrum. *Environmental Toxicology and Chemistry*,
472 **31**, 2099–2107.

MacFayden, E.J., Williamson, C.E., Grad, G., Lowery, M., Jeffrey, W.H. & Mitchell, D.L. (2004) Molecular response to climate change: temperature dependence of UV-induced DNA damage and repair in the freshwater crustacean *Daphnia pulicaria*. *Global Change Biology*, **10**, 408–416.

Malloy, K.D., Holman, M.A., Mitchell, D. & Detrich III, H.W. (1997) Solar UVB-induced DNA damage and photoenzymatic DNA repair in antarctic zooplankton. *Proceedings of the National Academy of Sciences of the United States of America*, **94**, 1258–1263.

Marchesi, E., Rota, C., Fann, Y.C., Chignell, C.F. & Mason, R.P. (1999) Photoreduction of the fluorescent dye 2',7'-dichlorofluorescein: a spin trapping and direct electron spin resonance study with implications for oxidative stress measurements. *Free Radical Biology and Medicine*, **26**, 148–161.

Martins, M. & Costa, P.M. (2015) The comet assay in environmental risk assessment of marine pollutants: applications, assets and handicaps of surveying genotoxicity in non-model organisms. *Mutagenesis*, **30**, 89–106.

Menzel, S., Bouchnak, R., Menzel, R. & Steinberg, C.E.W. (2011) Dissolved humic substances initiate DNA-methylation in cladocerans. *Aquatic Toxicology*, **105**, 640–642.

Miner, B.E. & Kerr, B. (2011) Adaptation to local ultraviolet radiation conditions among neighbouring *Daphnia* populations. *Proceedings of the Royal Society B: Biological Sciences*, **278**, 1307–1313.

Miner, B.E., Kulling, P.M., Beer, K.D. & Kerr, B. (2015) Divergence in DNA photorepair efficiency among genotypes from contrasting UV radiation environments in nature. *Molecular Ecology*, **24**, 6177–6187.

497 Mirbahai, L. & Chipman, J.K. (2014) Epigenetic memory of environmental
498 organisms: A reflection of lifetime stressor exposures. *Mutation Research/Genetic*
499 *Toxicology and Environmental Mutagenesis*, **764–765**, 10–17.
500 Moeller, R.E., Gilroy, S., Williamson, C.E., Grad, G. & Sommaruga, R. (2005)
501 Dietary acquisition of photoprotective compounds (mycosporine-like amino acids,
502 carotenoids) and acclimation to ultraviolet radiation in a freshwater copepod.
503 *Limnology and Oceanography*, **50**, 427–439.
504 Monteith, D.T., Stoddard, J.L., Evans, C.D., de Wit, H.A., Forsius, M., Høgåsen, T.,
505 Wilander, A., Skjelkvåle, B.L., Jeffries, D.S., Vuorenmaa, J., Keller, B., Kopácek,
506 J. & Vesely, J. (2007) Dissolved organic carbon trends resulting from changes in
507 atmospheric deposition chemistry. *Nature*, **450**, 537–540.
508 Mortensen, A. Skibsted, L.H., Sampson, J., Rice-Evans, C. & Everett, S.A. (1997)
509 Comperative mechanisms and rates of free radical scavenging by carotenoid
510 antioxidants, *FEBS Letters*, **418**, 91–97.
511 Palen, W.J., Schindler, D.E., Adams, M.J., Pearl, C.A., Bury, R.B. & Diamond, S.A.
512 (2002) Optical characteristics of natural waters protect amphibians from UV-B in
513 the US Pacific Northwest. *Ecology*, **83**, 2951–2957.
514 Pellacani, C., Buschini, A., Furlini, M., Poli, P. & Rossi, C. (2006) A battery of *in*
515 *vivo* and *in vitro* tests useful for genotoxic pollutant detection in surface waters.
516 *Aquatic Toxicology*, **77**, 1–10.
517 Pellegri, V., Gorbi, G. & Buschini, A. (2014) Comet assay on *Daphnia magna* in eco-
518 genotoxicity testing. *Aquatic Toxicology*, **155**, 261–268.
519 Pinheiro, J.C. & Bates, D.M. (2000) *Mixed-effect models in S and S-PLUS*. Springer,
520 New York.

Pinheiro, J.C., Bates, D.M., DebRoy, S., Sarkar, D. & R Core Team. (2016) nlme: Linear and nonlinear mixed effects models. R package version 3.1-128. https://CRAN.R-project.org/package=nlme

R Core Team. (2016) R: A language and environment for statistical computing. R Foundation for Statistical Computing, Vienna, Austria. https://www.R-project.org/

Rae, R., Howard-Williams, C., Hawes, I., Schwarz, A.-M. & Vincent, W.F. (2001) Penetration of solar ultraviolet radiation into New Zealand lakes: influence of dissolved organic carbon and catchment vegetation. *Limnology*, **2**, 79–89.

Rhode, S.C., Pawlowski, M. & Tollrian, R. (2001) The impact of ultraviolet radiation on the vertical distribution of zooplankton of the genus *Daphnia*. *Nature*, **412**, 69–72.

Richard, L.E., Peake, B.M., Rusak, S.A., Cooper, W.J. & Burritt, D.J. (2007) Production and decomposition dynamics of hydrogen peroxide in freshwater. *Environmental Chemistry*, **4**, 55–64.

Robinson, S.A. & Erickson III, D.J. (2015) Not just sunburn – the ozone hole's profound effect on climate has significant implications for Southern Hemisphere ecosystems. *Global Change Biology*, **21**, 515–527.

Schindler, D.W., Curtis, P.J., Bayley, S.E., Parker, B.R., Beaty, K.G. & Stainton, M.P. (1997) Climate-induced changes in the dissolved organic carbon budgets of boreal lakes. *Biogeochemistry*, **36**, 9–28.

Scoville, A.G. & Pfrender, M.E. (2010) Phenotypic plasticity facilitates recurrent rapid adaptation to introduced predators. *Proceedings of the National Academy of Sciences of the United States of America*, **107**, 4260–4263.

544 Scully, N.M., McQueen, D.J. & Lean, D.R.S. (1996) Hydrogen peroxide formation:
545 the interaction of ultraviolet radiation and dissolved organic carbon in lake waters
546 along a 43–75°N gradient. *Limnology and Oceanography* **41**, 540–548.
547 Seekell, D.A., Lapierre, J.-F. & Karlsson, J. (2015) Trade-offs between light and
548 nutrient availability across gradients of dissolved organic carbon concentration in
549 Swedish lakes: implications for patterns in primary production. *Canadian Journal*
550 *of Fisheries and Aquatic Sciences*, **72**, 1663–1671.
551 Singh, N.P., McCoy, M.T., Tice, R.R. & Schneider, E.L. (1988) A simple technique
552 for quantitation of low levels of DNA damage in individual cells. *Experimental*
553 *Cell Research*, **175**, 184–191.
554 Sinha, R.P. & Häder, D.-P. (2002) UV-induced DNA damage and repair: a review.
555 *Photochemical and Photobiological Sciences*, **1**, 225–236.
556 Skibsted, L.H. (2012) Carotenoids in antioxidant networks: colorants or radical
557 scavengers. *Journal of Agricultural and Food Chemistry*, **60**, 2409–2417.
558 Solomon, C.T., Jones, S.E., Weidel, B.C., Buffam, I., Fork, M.L., Karlsson, J.,
559 Larsen, S., Lennon, J.T., Read, J.S., Sadro, S. & Saros, J.E. (2015) Ecosystem
560 consequences of changing inputs of terrestrial dissolved organic matter to lakes:
561 current knowledge and future challenges. *Ecosystems*, **18**, 376–389.
562 Sommaruga, R. & Garcia-Pichel, F. (1999) UV-absorbing mycosporine-like
563 compounds in planktonic and benthic organisms from a high-mountain lake.
564 *Archiv für Hydrobiologie*, **144**, 255–269.
565 Sprent, P. & Dolby, G.R. (1980) Query: The geometric mean functional relationship.
566 *Biometrics*, **36**, 547–550.

567 Tartarotti, B., Baffico, G., Temporetti, P. & Zagarese, H.E. (2004) Mycosporine-like
568 amino acids in planktonic organisms living under different UV exposure
569 conditions in Patagonian lakes. *Journal of Plankton Research*, **26**, 753–762.
570 Tartarotti, B., Saul, N., Chakrabarti, S., Trattner, F., Steinberg, C.E.W. &
571 Sommaruga, R. (2014) UV-induced DNA damage in *Cyclops abyssorum tatricus*
572 populations from clear and turbid alpine lakes. *Journal of Plankton Research*, **36**,
573 557–566.
574 Thoma, F. (1999) Light and dark in chromatin repair: Repair of UV-induced DNA
575 lesions by photolyase and nucleotide excision repair. *The EMBO Journal*, **18**,
576 6585–6598.
577 Thrane, J.-E., Hessen, D.O. & Andersen, T. (2014) The absorption of light in lakes:
578 negative impact of dissolved organic carbon on primary productivity. *Ecosystems*,
579 **17**, 1040–1052.
580 Urabe, J., Kyle, M., Makino, W., Yoshida, T., Andersen, T. & Elser, J.J. (2002)
581 Reduced light increases herbivore production due to stoichiometric effects of
582 light/nutrient balance. *Ecology*, **83**, 619–627.
583 Vehmaa, A., Hogfors, H., Gorokhova, E., Brutemark, A., Holmborn, T. & Engström-
584 Öst, J. (2013) Projected marine climate change: effects on copepod oxidative status
585 and reproduction. *Ecology and Evololution*, **3**, 4548–4557.
586 Williamson, C.E., Zagarese, H.E., Schulze, P.C., Hargreaves, B.R. & Seva, J. (1994)
587 The impact of short-term exposure to UV-B radiation in zooplankton communities
588 in north temperate lakes. *Journal of Plankton Research*, **16**, 205–218.
589 Williamson, C.E., Neale, P.J., Grad, G., de Lange, H.J. & Hargreaves, B.R. (2001)
590 Beneficial and detrimental effects of UV on aquatic organisms: implications of
591 spectral variation. *Ecological Applications*, **11**, 1843–1857.

592 Williamson, C.E., Overholt, E.P., Pilla, R.M., Leach, T.H., Brentrup, J.A., Knoll,
593 L.B., Mette, E.M. & Moeller, R.E. (2015) Ecological consequences of long-term
594 browning in lakes. *Scientific Reports*, **5**, 10 pp.
595 Wilson, C.L., Hinman, N.W. & Sheridan, R.P. (2000) Hydrogen peroxide formation
596 and decay in iron-rich geothermal waters: the relative roles of abiotic and biotic
597 mechanisms. *Photochemistry and Photobiology*, **71**, 691–699.
598 Yan, N.D., Keller, W., Scully, N.M., Lean, D.R.S. & Dillon, P.J. (1996) Increased
599 UV-B penetration in a lake owing to drought-induced acidification. *Nature*, **381**,
600 141–143.
601 Zagarese, H.E., Tartarotti, B. & Añón Suárez, A. (2003) The significance of
602 ultraviolet radiation for aquatic organisms. *Modern Trends in Applied Aquatic*
603 *Ecology* (eds R.S. Ambasht & N.K. Ambasht), pp. 173–200. Springer International
604 Publishing, New York City, NY, USA.

Supporting Information

Additional Supporting information may be found in the online version of this article:

Figure S1. Principal mechanistic pathway of the DCFH-DA ROS production assay.

Appendix S1. Comet assay data and R script to analyse the effects of DOC and UVA_{390} on DNA damage.

Appendix S2. Raw ROS production data and R script to summarise ROS production.

Appendix S3. Absorbance data and R script to analyse the effects of DOC, UVA_{390}, and absorbed photons on ROS production.

Appendix S4. R script to analyse the effects of ROS production on DNA damage.

Figure legends

Fig. 1. Response-surface plot of DOC and UVA_{390} effects on DNA damage in *D. magna*. The surface was obtained from a LME model with DNA damage as response variable, DOC, UVA_{390} and their interaction as fixed effect, and individual daphnids and experimental as random factor with individual daphnids nested in their experimental replicates. $n = 141$.

Fig. 2. Correlation of absorbed photons and ROS production. The three distinct groups can be attributed to 0, 21.7, and 43.4 μmol UVA_{390} m^{-2} s^{-1} (squares, circles, and triangles, respectively). Within these groups, the four values represent 2.03, 5, 10, and 20 mg DOC L^{-1} (left to right). Both dimensions are directly comparable, i.e., mmol m^{-3} = μmol L^{-1}. $n = 36$. Dots: mean values for each treatment ± standard error; red line: LME model prediction; red band: 95% confidence interval; right-hand rugs: raw ROS production data distribution.

Fig. 3. Comet assay results of all DOC×UVA_{390} treatments expressed as a function of ROS production in respective treatments. The LME model regression was obtained by major axis regression using both variables (DNA damage and ROS production) as fixed effects, and subsequently using the geometric mean of both LME models. n = 141 and 36, respectively. Dots: mean values for each treatment ± standard error; red line: LME model prediction; red band: 95% confidence interval; upper rug: raw ROS production distribution; right-hand rug: raw DNA damage data distribution.

Table legends

Tab. 1. Summary of comet assay results for *D. magna* exposed to DOC and UVA_{390}. Results are expressed as mean DNA damage ± standard error of three independent experiments.

Tab. 2. Summary of *in vitro* ROS formation rates for DOC and UVA_{390} combinations. Results are expressed as mean ROS formation rate ± standard error of three independent experiments.

Figures

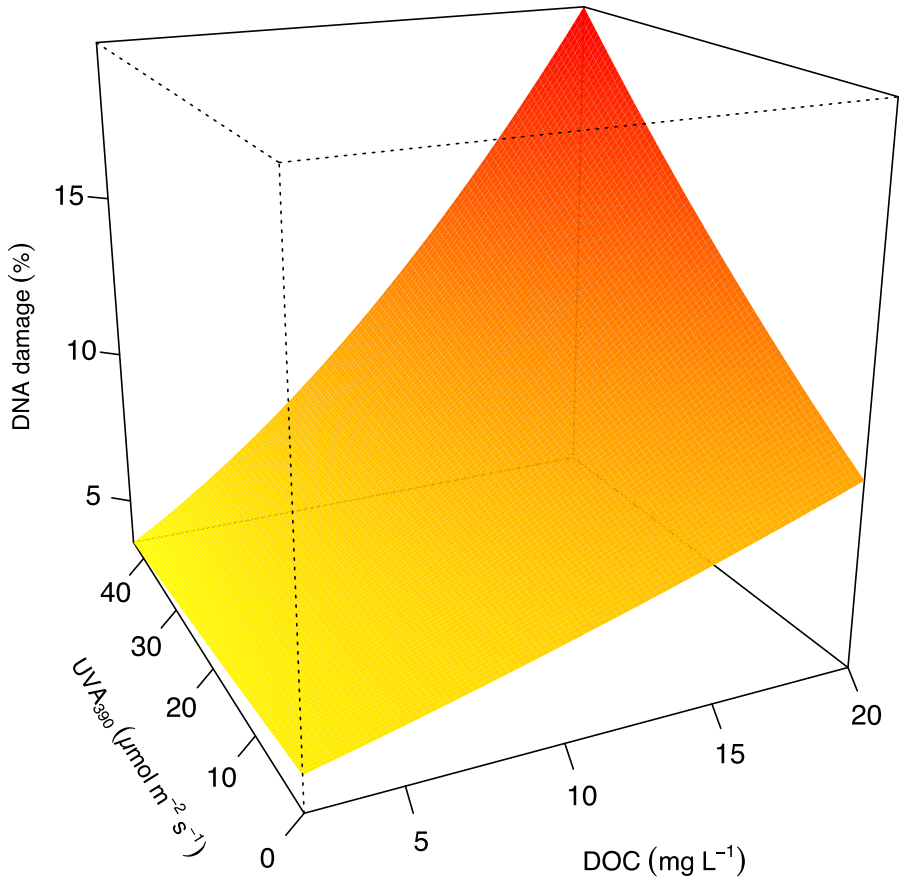

Fig. 1

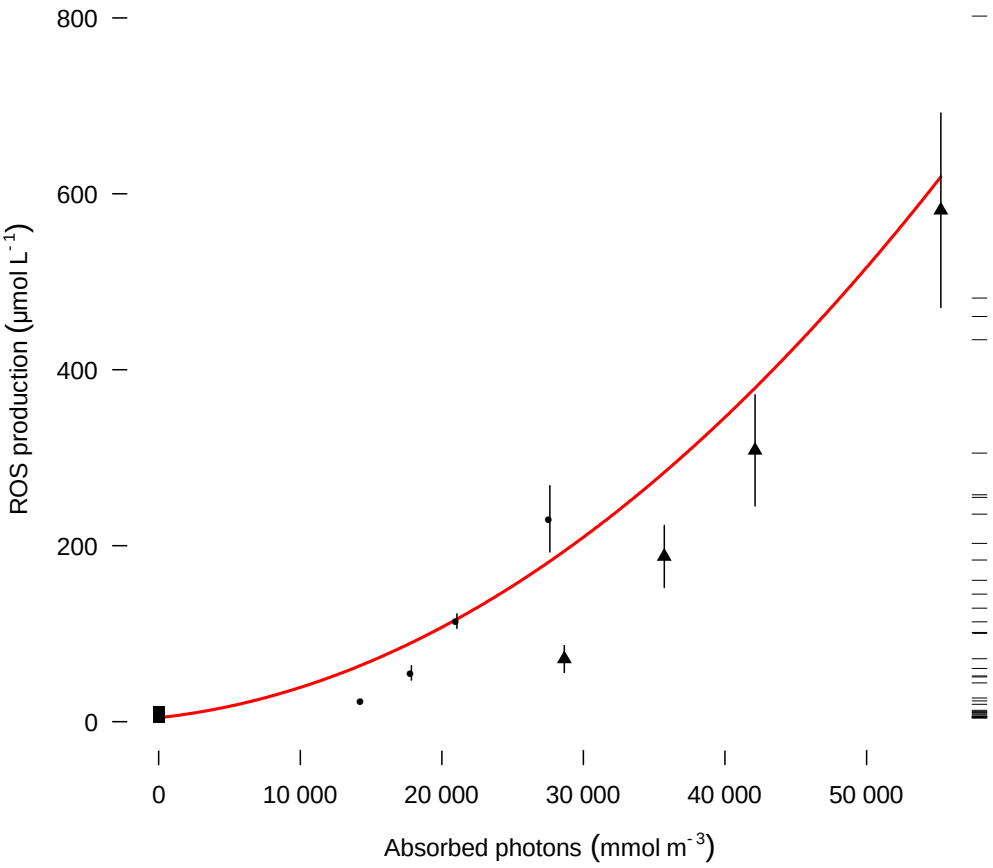
800
600
400
200
0
ROS production (µmol L-1)
0
10 000
20 000
30 000
40 000
50 000
Absorbed photons (mmol m-3)

644

645 **Fig. 2**

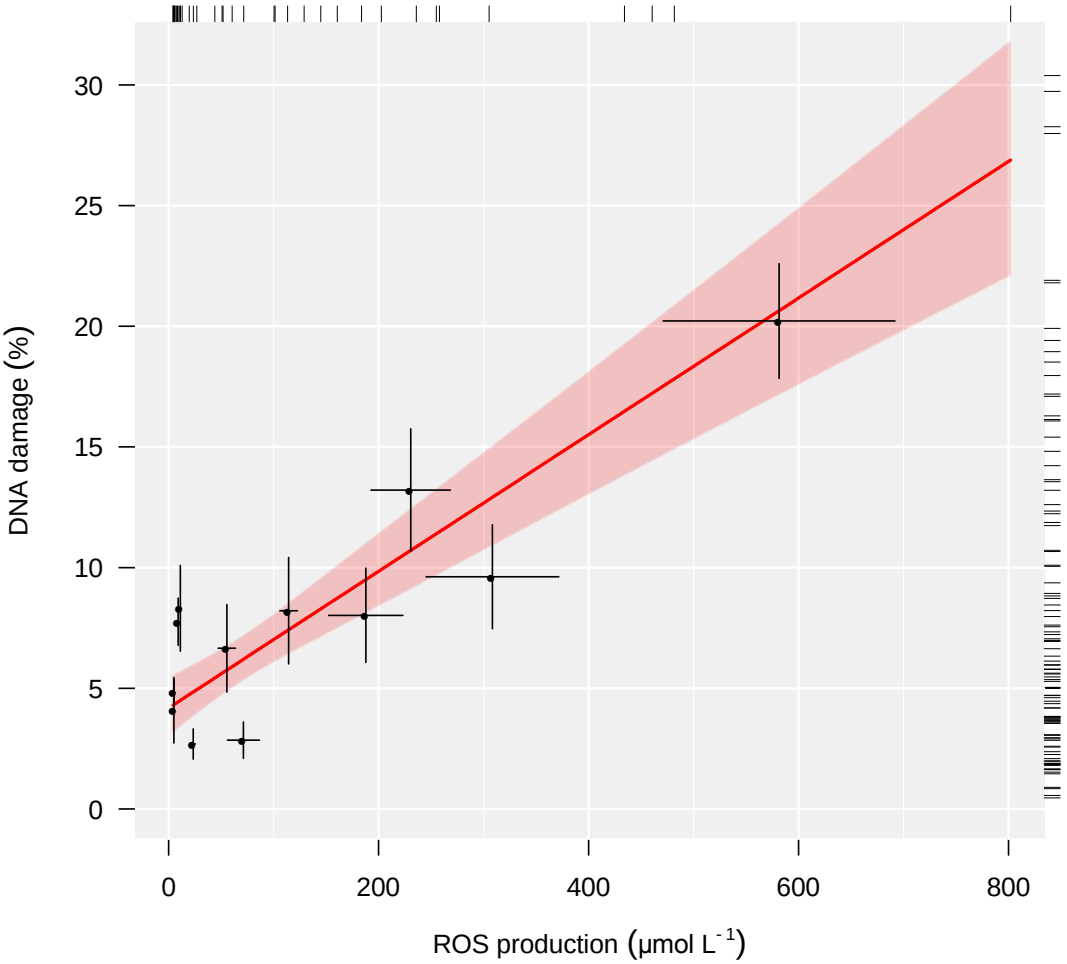
DNA damage (%)
0
5
10
15
20
25
30
0
200
400
600
800
ROS production (µmol L-1)

646

647 **Fig. 3**

Tables

Table 1

DOC	UVA_{390}			
	0 µmol m^{-2} s^{-1}	10.8 µmol m^{-2} s^{-1}	21.7 µmol m^{-2} s^{-1}	43.4 µmol m^{-2} s^{-1}
2.03 mg L^{-1}	4.1±1.4%	4.5±0.7%	2.7±0.6%	2.9±0.8%
5.0 mg L^{-1}	4.8±0.5%	8.8±0.8%	6.7±1.8%	8.0±1.9%
10.0 mg L^{-1}	7.8±1.0%	9.8±1.3%	8.2±2.2%	9.6±2.2%
20.0 mg L^{-1}	8.3±1.8%	13.2±2.5%	13.2±2.5%	20.2±2.4%

651 **Table 2**

DOC	UVA_{390}		
	0 μmol m^{-2} s^{-1}	21.7 μmol m^{-2} s^{-1}	43.4 μmol m^{-2} s^{-1}
2.03 mg L^{-1}	5.1±0.6 μmol L^{-1}	23.4±2.1 μmol L^{-1}	71.3±15.3 μmol L^{-1}
5.0 mg L^{-1}	5.2±0.5 μmol L^{-1}	55.4±8.3 μmol L^{-1}	187.8±35.3 μmol L^{-1}
10.0 mg L^{-1}	9.1±1.1 μmol L^{-1}	114.3±8.3 μmol L^{-1}	308.4±63.2 μmol L^{-1}
20.0 mg L^{-1}	11.1±1.0 μmol L^{-1}	230.5±37.8 μmol L^{-1}	581.4±110.5 μmol L^{-1}

652